Alphavirus RNA Replicase Is Located on the Cytoplasmic Surface of Endosomes and Lysosomes

Susan Froshauer, Jürgen Kartenbeck, and Ari Helenius

Department of Cell Biology, Yale University School of Medicine, New Haven, Connecticut 06510

Abstract. Using morphological and cell biological techniques, we have shown that the RNA replicase of Semliki Forest and Sindbis virus (two closely related alphaviruses) is located in complex ribonucleoprotein structures associated with the cytoplasmic surface of modified secondary lysosomes and endosomes. These nucleoprotein complexes often form a bridge between the membrane of the endocytic vacuole and the rough endoplasmic reticulum where the synthesis of the structural proteins of these viruses occurs. The results suggest that these cytopathic vacuoles constitute sites not only for viral RNA synthesis, but also for translation of structural proteins, and for the assembly of nucleocapsids.

DURING the initial stages of virus infection, the genome and accessory proteins of incoming virions are delivered into the cytosol of the animal cell. Penetration into the cytosol occurs, as a rule, through the plasma membrane or the membrane of endocytic vacuoles. Subsequent uncoating of the genome and replication takes place either in the nucleus, in association with cytoplasmic organelles, or in soluble cytoplasmic complexes. In many cases cellular factors appear to be needed in the early cytosolic processes. While the mechanisms of penetration and the molecular events during replication are increasingly well understood for many viruses, little is now known about nucleocapsid uncoating, intracytoplasmic relocation, transport to the nucleus, and association with intracellular proteins and organelles.

In this paper we address the cell biology of the early cytoplasmic events during Semliki Forest virus (SFV)[1] and Sindbis virus infection. These alphaviruses are known to enter cells by receptor-mediated endocytosis via coated pits, followed by acid-activated membrane fusion in the endosomal compartment (see Kielian and Helenius, 1986). As a result the nucleocapsid, an isometric spherical particle composed of a single-stranded RNA molecule and 240 copies of a single capsid protein (Fuller, 1987), is released into the cytoplasm. The subsequent replication of alphaviral RNA occurs entirely within the cytoplasmic compartment in association with cytoplasmic organelles (see Strauss and Strauss, 1986).

The starting point for these studies was a group of observations made some twenty years ago by Acheson and Tamm (1967), Grimley et al. (1968), and Friedman et al. (1972), which showed that alphavirus-infected cells contained morphologically distinct cytopathic vacuoles. Some of these, the so-called cytopathic vacuoles I (CPVs), were implicated as the organelles of RNA replication (Grimley et al., 1968; Friedman et al., 1972). CPVs were identified by EM as complex vacuolar structures, 0.6–2.0 μm in diameter, equipped with characteristic 50-nm light bulb-shaped membrane spherules lining the limiting membrane at regular intervals. However, given the limitations of the techniques available at the time, the correlation between the CPVs and RNA replication remained tentative, and the origin and nature of the vacuoles unknown (Grimley et al., 1972; Friedman et al., 1972).

The results presented in this paper show that CPVs are endosomes and lysosomes modified by association of virus-specific components. The viral RNA polymerase is present in large, branching, granular, and fibrous structures anchored to the cytoplasmic surface of CPVs at the spherules. A connection between CPVs and the rough endoplasmic reticulum (RER) via these structures was also observed. Taken together, the results explain some of the key events during the early stages of the replication cycle. Furthermore, they suggest that translation, transcription, and assembly of viral nucleocapsids may occur within a single large CPV-associated cytoplasmic structure.

Materials and Methods

Virus and Cell Cultures

SFV was grown from a plaque-purified stock derived from the prototype Helsinki strain as described by Kääriäinen et al. (1969) and Kielian et al. (1984). Infection and cell maintenance procedures have been described (Helenius et al., 1980, 1982; Schmid et al., 1988). Identical procedures were followed for propagation of Sindbis virus, a gift of Bart Sefton (The Salk Institute, San Diego, CA).

Jürgen Kartenbeck's present address is Institute of Cell and Tumor Biology, German Cancer Research Center, Heidelberg, FRG.

1. *Abbreviations used in this paper*: CPV, cytopathic vacuoles I; MOI, multiplicity of infection; RER, rough endoplasmic reticulum; SFV, Semliki Forest virus.

Antibodies

Rabbit polyclonal anti-nsP1, nsP2, nsP3, and nsP4 antisera recognize SFV and Sindbis virus nonstructural proteins by immunoprecipitation (Hardy and Strauss, 1988). Anti-nsP3 and nsP4 sera also recognize Sindbis antigens by immunofluorescence (this communication). Rabbit polyclonal anti-lgp110 and anti-lgp120 antisera and affinity-purified rat monoclonal anti-lgp110 IgG (GL2A7 Kn) have been described (Lewis et al., 1985; Green et al., 1987). Mouse monoclonal anti-lgp96 IgG (E9A4) recognizes lgp96 in Chinese hamster ovary (CHO) cells (S. Schmid, R. Fuchs, K.-P. Zimmer, and I. Mellman, Yale University Medical School, New Haven, CT). Rabbit polyclonal anti-cathepsin L recognizes cathepsin L in NIH3T3 and CHO cells.

Affinity-purified goat anti-rabbit IgG, and rhodamine-conjugated goat anti-rat IgG were purchased from Tago Inc. (Burlingame, CA). Peroxidase-conjugated sheep anti-mouse and anti-rabbit Fab fragments were from BIO-SYS (Pasteur Institute, Paris, France). 5- and 10-nm gold-conjugated goat anti-rabbit and anti-mouse IgGs were from Janssen Pharmaceutica (Beerse, Belgium).

Metabolic Radiolabeling of Viral RNA and Proteins

Pulse-labeled viral RNA was produced by treating cells for 1 h, 3.5 h after infection with 2 μg/ml actinomycin D (Worthington Biochemical Corp., Freehold, NJ), then pulse labeling for 3 min with 500 μCi [^{3}H]uridine (New England Nuclear, Boston, MA)/7 × 10^7 cells in prewarmed serum-free MEM with 2 μg/ml of actinomycin D. Dishes were placed on ice and washed three times with ice-cold PBS containing 10 mM uridine. To label viral proteins, cells were incubated in methionine-free medium containing 2 μg/ml actinomycin D for 30 min, 1 h after infection. Cells were labeled with 0.75 mCi [^{35}S]methionine (Amersham Corp., Arlington Heights, IL; 3,300 Ci/mmol)/7 × 10^7 cells.

Free-flow Electrophoresis

Virus-infected CHO cell homogenates were prepared from 1 × 10^8 cells according to the method of Marsh et al. (1987) and Balch and Rothman (1985). Under these conditions the majority of nuclei remain intact and 80% of the cells are lyzed.

Microsomes were prepared from postnuclear supernatants and resuspended to 1 mg/ml protein. Before electrophoresis, microsomes were treated with 10 μg/ml of TPCK-trypsin (Worthington Biochemical Corp.) for 5 min at 37°C, followed by treatment with 50 μg/ml of soybean trypsin inhibitor (Sigma Chemical Co., St. Louis, MO). Free-flow electrophoresis was performed using the Bender and Hobein ElphorVap21 instrument (Protein Technologies, Inc., Tucson, AZ) at 130 mA and 1,700–1,800 V as described (Marsh et al., 1987).

Protein, RNA, and Enzyme Assays

Protein was determined using the Coomassie Blue-binding assay (Bradford, 1976) or by monitoring radioactivity when cells were labeled with [^{35}S]methionine. [^{3}H]uridine RNA was detected by monitoring TCA-precipitable radioactivity. Marker enzymes β-hexosaminidase and alkaline phosphodiesterase were assayed fluorometrically according to Pool et al. (1983) and Hawley et al. (1981) to locate lysosomes and plasma membrane, respectively.

Immunoprecipitation of Sindbis Nonstructural Proteins

Pooled fractions obtained by free-flow electrophoresis were collected onto 1 M sucrose cushions by centrifugation at 28,000 rpm (SW28) for 35 min (4°C), and pellets were resuspended in lysis buffer (1 mM PMSF, 10 μg/ml leupeptin, 2 mM EDTA, and 1% NP-40 or 0.5% SDS in PBS).

4 vol of immunoprecipitation buffer (50 mM Tris, pH 7.4, 300 mM NaCl, 4 mM EDTA, 0.5% Triton X-100, 200 μg/ml BSA, and 40 μg/ml PMSF) were added to resuspended free-flow electrophoresis pellets or cell lysates and incubated for 1.5 h (0°C) in the presence of 2 μl of rabbit anti-nsP antibody. 100 μl of a 10% prewashed suspension of fixed *Staphylococcus aureus* (vol/vol in immunoprecipitation buffer; Zysorbin, Zymed Labs, San Francisco, CA) and 10 μl of goat anti-rabbit IgG were added before shaking samples for 1.5 h (4°C). Immune complexes were pelleted, washed three times in HSA (0.6 M NaCl, 0.125 M KH_2PO_4, pH 7.4, containing 0.02% Na azide), once in H_2O, resuspended in Laemmli sample buffer, and heated for 15 min at 65°C.

Gel Electrophoresis

SDS-PAGE was carried out under reducing conditions using 10% (wt/vol) polyacrylamide gels (Laemmli, 1970). Gels were stained with Coomassie Blue to detect high molecular mass standards (Sigma Chemical Co.) and enhanced with 1 M sodium salicylate for fluorography (Chamberlin, 1979).

Indirect Immunofluorescence Microscopy

Cells grown on multiwell slides (Carlson Scientific, Inc., Peotone, IL) were methanol fixed for 10 min or Nakane fixed for 1 h (McLean and Nakane, 1974), both at 0°C. Nakane-fixed cells were permeabilized with 0.005% saponin. Incubations with rabbit anti-nsP3 (or nsP4) sera (1:500) and fluorescein-conjugated goat anti-rabbit IgG (1:40) were for 30 min (25°C). Rabbit anti-nsP antisera were preadsorbed to fixed, uninfected cells. Cells mounted in moviol were photographed in a Photomicroscope III (Carl Zeiss, Inc., Thornwood, NY) equipped with epifluorescence.

Electron Microscopy

For thin-section electron microscopy, infected cells were fixed in 2.5% glutaraldehyde in cacodylate buffer (50 mM sodium cacodylate, pH 7.2, 50 mM KCl, and 2.5 mM $MgCl_2$) for 10 min. Cells were stained, dehydrated, detached from dishes with 100% propylene oxide, and embedded in Epon as described (Helenius et al., 1980). Ultrathin sections were examined at 60 kV in an electron microscope (100-CX; JEOL USA, Peabody, MA) after staining with uranyl acetate and/or lead citrate.

Immunoperoxidase cytochemistry was performed using the procedure of Brown and Farquhar (1984). Infected cells were fixed for 6 h (25°C) using Nakane's fixative permeabilized with 0.001% saponin, and incubated 12 h (0°C) with primary antibodies (anti-lgp120 [1:200], anti-lgp96 [1:100], or anti-cathepsin L IgG [1:50]), followed by incubation for 1.5 h (25°C) with peroxidase-conjugated sheep anti-rabbit Fab fragments (1:50). Subsequently, cells were fixed in 2.5% glutaraldehyde and treated with 50 mM Tris, pH 7.4, containing 7.5% sucrose, 0.2% diaminobenzidine hydrochloride, and 0.01% hydrogen peroxide for 3–10 min, postfixed, and embedded as described.

To examine free-flow electrophoresis fractions β-hexosaminidase and bulk protein peak fractions were collected into four 24-ml pools and fixed in glutaraldehyde (final concentration, 2.5%). After fixation (30 min, 25°C), fractions were pelleted at 28,000 rpm (SW28, 30 min, 4°C) onto a 1 M sucrose cushion. The sucrose cushion was resuspended in cacodylate buffer, and the membrane vesicles repelleted in an Eppendorf centrifuge for 15 min.

Morphometric analyses of thin sections obtained from the pelleted pools were performed according to the method of Weibel (1969). The total membrane surface area in each pool was determined by measuring intersections of the limiting membrane of CPVs or vacuoles with a grid placed over the photomicrographs of the sections. The measurements were normalized to relative amounts of total protein recovered in the fractions. A total of 2,640 intersections of CPVs compared to 5,188 for all other vacuoles was determined.

Uptake of Fluid Phase Markers

Cationic ferritin (Sigma Chemical Co.) was prepared as described (Nilsson et al., 1983) and added to cells at a final concentration of 0.5 mg/ml and horseradish peroxidase (Sigma) at 10 mg/ml. Horseradish peroxidase was visualized histochemically by fixing cells with 2.5% glutaraldehyde in cacodylate buffer and treating with diaminobenzidine (see above).

Immunogold Labeling of Semi-intact Cells

The procedure of Beckers et al. (1978) was followed to render CHO cells semi-intact by the nitrocellulose technique. 70–80% of the cells were disrupted based on trypan blue permeability. Permeabilized cells were fixed in 3% fresh formaldehyde in PBS for 20 min on ice and incubated with anti-nsP3 or nsP4 antibodies (1:100) for 1.5 h (25°C), followed by incubation with 5-nm gold-conjugated goat anti-rabbit IgG (1:100) for 4 h (25°C).

Immunogold Labeling of Saponin-permeabilized Cells

CHO cells were Nakane fixed for 2.5 h, and permeabilized with 0.1 or 0.5% saponin for 10 min. Either rabbit anti-nsP3 (or nsP4) antibodies or mouse anti-lgp96 IgG (1:100) were added for 2.5h, followed by incubation with 5-nm gold-conjugated goat anti-rabbit IgG for single-labeling experiments

or 10-nm gold-conjugated goat anti-rabbit IgG (1:10) with 5-nm gold-conjugated goat anti-mouse IgG (1:10) for double-labeling. Secondary antibodies were added for 12 h (4°C). All other incubations were performed at 25°C.

Results

Ultrastructure of CPVs

The morphology of CPVs has been described previously in detail (Acheson and Tamm, 1967; Grimley et al., 1968, 1972). Our electron micrographs of infected baby hamster kidney (BHK) and CHO cells are well in agreement with previous studies (Fig. 1). Although quite heterogenous with respect to size and internal contents, the CPVs were easily recognized by the charateristic spherules associated with the limiting membrane. We found they were distributed throughout the cytosol, but were often located in close proximity to elements of the RER (Fig. 1 *a*).

Although the previous studies have suggested that CPVs are either derived from the Golgi apparatus or from mitochondria (Grimley et al., 1972; Friedman et al., 1972), we found that they looked more similar to lysosomes and endosomes (Fig. 1, *a*, *b*, and *g*). For example, they contained multivesicular inclusions, amorphous material, and occasional intact-looking virions. That the spherules represented invaginations of the limiting membrane of the vacuoles was clearly seen in fortuitous sections (*arrowhead*, Fig. 1 *b*). Inside the spherule a dense, star-shaped structure was often seen with thin spokes radiating from a central mass (Fig, 1, *b–e*). The narrow, membranous neck of the spherule (outer diameter, 19–20 nm; inner diameter, 8 nm) typically contained an electron dense plug (*arrow*, Fig. 1 *c*). The plug was sometimes connected to electron dense material extending into the cytoplasm (*large arrowhead*, Fig. 1, *b–d*). In some images this material had a threadlike appearance, and it often contained granules which corresponded in size and morphology to ribosomes and to nucleocapsids (Fig, 1, *c* and *d*).

Clusters of spherules were present on the plasma membrane, and occasionally a spherule could be seen in a coated pit or a coated vesicle suggesting that it was being endocytosed (Fig. 1 *h*). Images in which CPVs appeared to fuse with the plasma membrane suggested that intracellular CPVs could be the source of the plasma membrane spherules (Fig. 1 *f*).

We observed that CPVs became detectable after 1 h of infection at moderately high multiplicity (multiplicity of infection [MOI] = 200) (Table I). The CPVs observed at this early time point had endosome-like morphology and only a few spherules (Fig. 1 *g*). At 5 h, when the cells reached a maximum level of virus production (and were probably already superinfected with progeny virus), numerous mature CPVs appeared. These had many spherules and a lysosome-like appearance (Fig. 1, *a* and *b*). The concentration of early CPVs was clearly dependent on MOI because if a low multiplicity were used (MOI = 20), CPVs became detectable only after 5 h of infection.

CPVs Are Modified Endosomes and Lysosomes

Since CPVs displayed so many morphological similarities with endosomes and lysosomes, we tested whether endocytosed substances were delivered to them. As shown in Fig. 2 *a*, two commonly used, nonspecific endocytic tracers, cationic ferritin and horseradish peroxidase, were internalized into the lumen of CPVs when added to the medium of infected cells. When the tracers were present for 2 h beginning 5 h after infection, 60% of the CPVs in CHO cells became labeled. The extent of labeling of individual CPVs was quite variable, but this was true for endosomes and lysosomes in uninfected cells as well. Inclusion into CPVs was also seen when cells were treated with the tracers 1 h before infection only. These results suggested that the CPVs were part of the endocytic pathway and that they originated through modification of preexisting endocytic vacuoles.

To examine whether some of the CPVs were endosomal, we determined whether CPVs could be labeled with cationic ferritin at 20°C. At this temperature endosomes can be labeled with endocytic tracers but delivery to lysosomes is blocked (Dunn et al., 1980; Marsh et al., 1983; Ukkonen et al., 1986). CHO cells were infected at 37°C for 2 h and then shifted to 20°C, and cationic ferritin was added for 1 h, 4 h after infection. It was found that a small fraction (~10%) of CPVs became labeled (data not shown). The labeled CPVs had structural features typical of endosomes, including the tubular extensions (Marsh et al., 1986). From this we concluded that a fraction of CPVs in CHO cells consisted of prelysosomal endocytic vacuoles.

Immunoperoxidase cytochemistry showed that the majority of CPVs were lysosomal. CPVs stained positively for four lysosomal marker antigens: lgp120, lgp110, lgp96, and cathepsin L (Fig. 2 *b*). The lgps are highly glycosylated, transmembrane proteins which are almost exclusively localized in lysosomal membranes of noninfected cells (Lewis et al., 1985; Green et al., 1987; Schmid, S., R. Fuchs, K.-P. Zimmer, and I. Mellman, personal communication) and cathepsin L is a lysosomal hydrolase. When infected CHO cells were immunolabeled with antibodies to lgp120, 90% of the organelles labeled were CPVs. In NIH3T3 cells infected with SFV, 40% of the organelles labeled by anti-lgp110 or anti-cathepsin L antibodies could be identified unambiguously as CPVs. Very few of the organelles stained with lgp120 were normal lysosomes indicating that a large fraction of lysosomes had been converted to CPVs after 5 h of infection.

Isolation of CPVs

The lysosomal nature of the majority of CPVs in CHO cells was consistent with their behavior during cell fractionation. When infected cells were subjected to the fractionation protocol used in our laboratory to isolate lysosomes, enrichment of CPVs was achieved. We used the free-flow electrophoresis method of Harms et al. (1980) as modified by Marsh et al. (1987). The method takes advantage of the anodal mobility of lysosomes in a strong electric field. CPVs were found to shift like lysosomes when subjected to this isolation protocol.

Microsomes prepared from SFV- or Sindbis-infected CHO cells were treated briefly with 1% trypsin for 1 mg/ml of protein (a treatment required for optimal separation of lysosomes from other organelles including endosomes) and applied to the free-flow electrophoresis machine as previously described (Marsh et al., 1987). Fig. 3 *a* shows the separation of the lysosomal marker β-hexosaminidase and total protein in a typical experiment. It was very similar to that obtained for uninfected CHO cells (data not shown; see

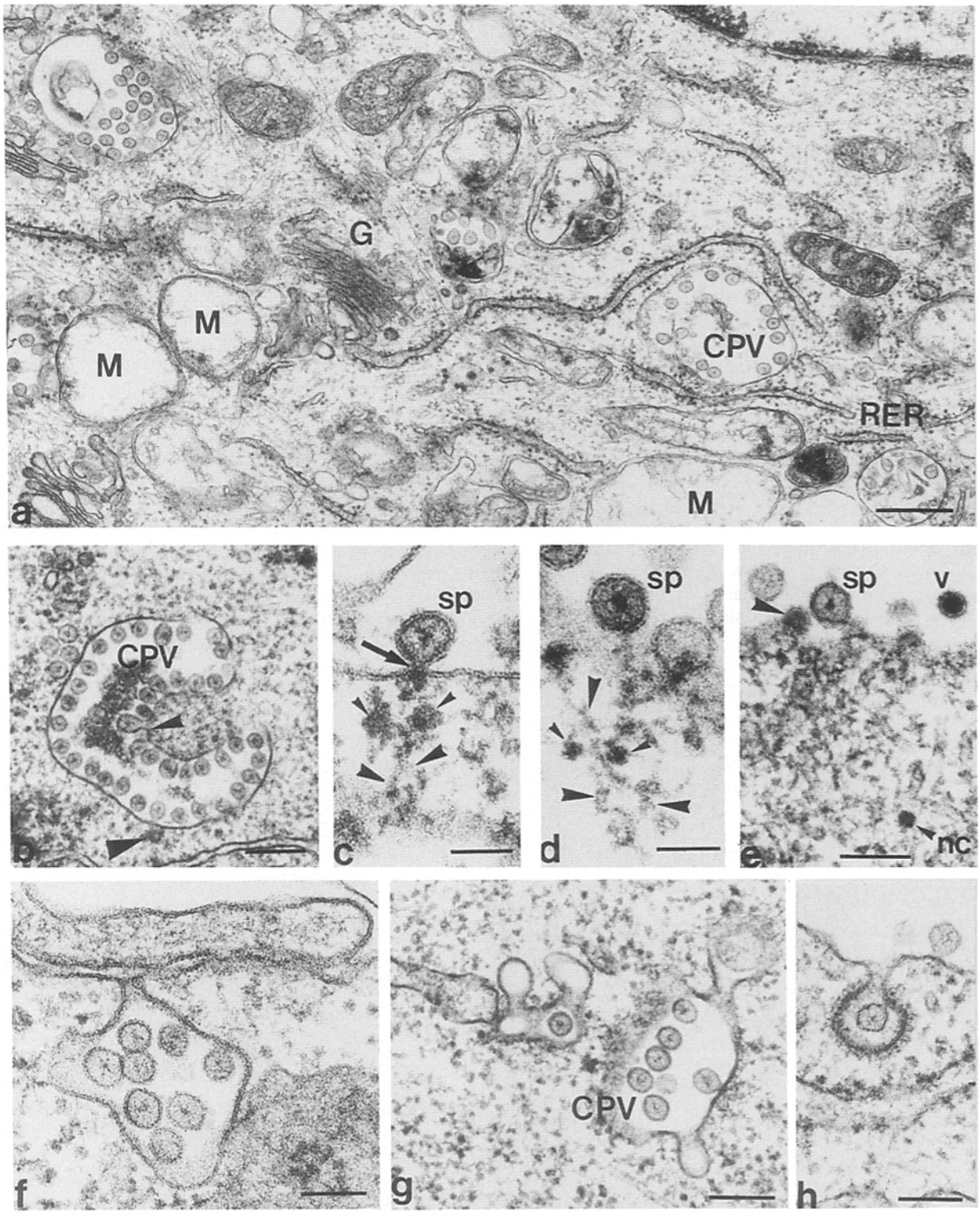

Figure 1. Ultrastructure of CPVs. BHK cells were infected with SFV for 2–5 h (MOI = 200) and examined by EM. (*a*) Overall distribution and membranous inclusions in CPVs showing lysosomal characteristics. The proximity of some CPVs to the RER can be seen. Spherules (50 nm) can be seen lining the membrane of CPVs. (*b*) The small arrowhead indicates the continuity of the spherule neck (outer diameter, 19–20 nm; inner diameter, 8 nm) with the vacuole membrane. The large arrowheads (*b–d*) indicate threadlike material attached to base of spherule at the electron dense plug (*arrow*; *c*). Granular material the size of ribosomes can be seen attached to the threads (*small arrowheads*; *c* and *d*). (*e*) A virion (*v*), spherules (*sp*), nucleocapsid (*nc*), and budding virus (*arrowhead*) are juxtaposed. (*f*) A vacuole with spherules is fused with the plasma membrane. (*g*) A CPV with tubular projections has the morphology of an endosome. (*h*) A spherule at the plasma membrane is in a coated pit. *N*, nucleus; *M*, mitochondria; *G*, Golgi apparatus; *sp*, spherule; *v*, virion; *nc*, nucleocapsid. Bars: (*a*) 391; (*b*) 217; (*c*) 103; (*d*) 83; (*e*) 131; (*f*) 137; (*g*) 157; and (*h*) 140 nm.

Table I. The Time Course of CPV Formation

Multiplicity of infection (MOI; pfu/cell)	Time postinfection	Presence of CPVs
	h	
20	3	−
	5	++
200	1	+
	2	++
	4	+++

BHK cells were infected with SFV and prepared for EM analysis as described in Materials and Methods. (−) CPVs were not detected; (+) CPVs rare; (++) CPVs obvious; or (+++) CPVs abundant.

Marsh et al., 1987; Schmid et al., 1988) resulting in a more than fourfold enrichment of the lysosomal marker in the most anodal peak over total microsomal pellet. Markers for mitochondria, plasma membrane, endoplasmic reticulum, and most of the Golgi membranes eluted in the main protein peak (data not shown; see Marsh et al., 1987; Schmid et al., 1988).

Thin-section electron micrographs of pellets made from the lysosome peak (pools I and II) and the main protein peak (pools III and IV) showed that CPVs were, indeed, highly enriched (Fig. 3 *b*). A morphometric analysis of the pools (normalizing against the protein content) showed that 70% of total CPVs were in pool II, and that 71% of the total membrane in pool II was in CPVs. Altogether the lysosomal peak contained 17% of total microsomal protein. Although lightly trypsin treated to allow the anodal shift of lysosomes, the CPVs retained most of their morphological characteristics. The spherules with their dense central structures and plugs at their necks were present. The electron dense threads that extend into the cytoplasm from the CPV membrane in intact cells were, however, absent.

The RNA Polymerase

The enrichment of CPVs in the lysosome peak after free-flow electrophoresis gave us an opportunity to determine directly whether the CPVs contained the RNA replication machinery. We determined whether the RNA polymerase subunits were present using specific polyclonal antibodies that recognize nonstructural proteins nsP1, 2, 3, and 4 of Sindbis virus (Hardy and Strauss, 1988). Although their individual roles have not been elucidated, the nsPs are known to be involved in viral RNA replication and processing, and they are thought to constitute subunits of the RNA polymerase complex. They are newly synthesized after penetration and are not components of incoming virions (Clewley and Kennedy, 1976; Ranki and Kääriänen, 1979; Gomatos et al., 1980; Keränen and Ruohonen, 1983; Strauss et al., 1983; Lopez et al., 1985; Hardy and Strauss, 1988).

We prepared microsomes from [^{35}S]methionine-labeled Sindbis-infected cells, subjected them to free-flow electrophoresis, and immunoprecipitated pooled fractions after solubilization with NP-40. As shown in Fig. 4, we found to our surprise that the fractions richest in CPVs contained the lowest amounts of nsP1, 2, 3, and 4. (Pools 2–5 in Fig. 4 are equivalent to pools I–IV, respectively, in Fig. 3 *a*). The

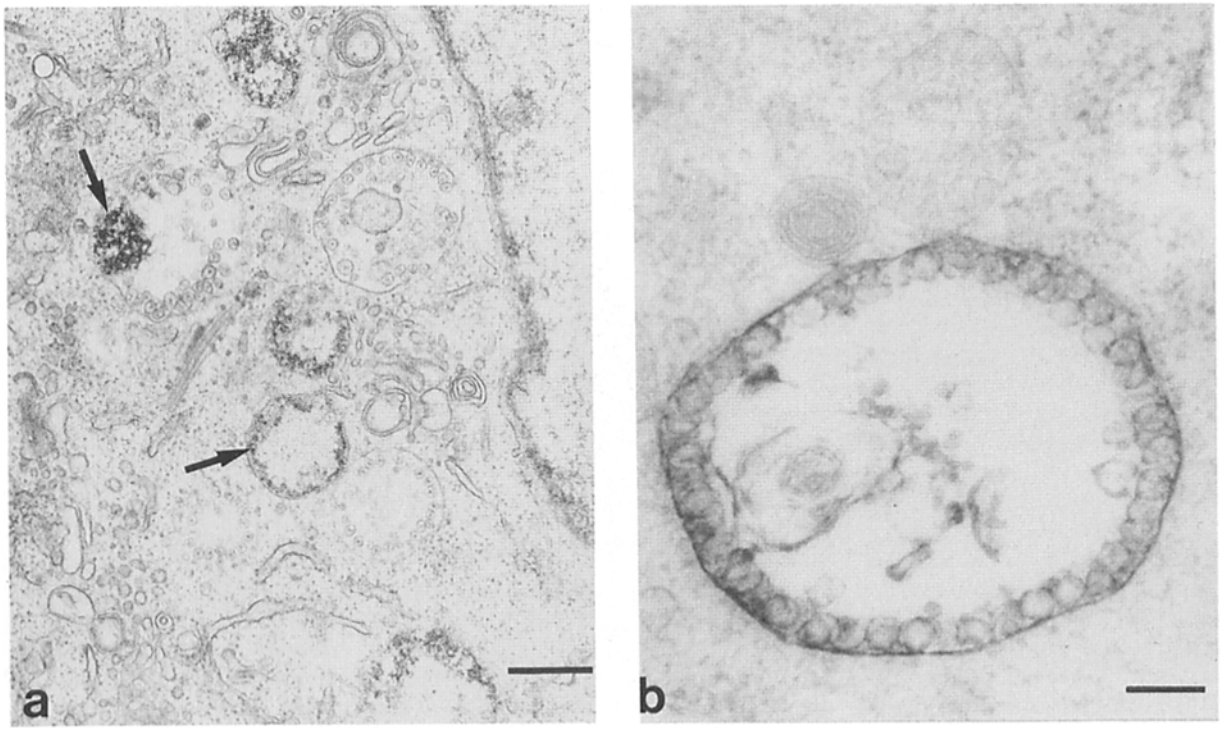

Figure 2. CPVs labeled with cationic ferritin or with immunoperoxidase using lgp120 antibodies. CHO cells were infected with SFV for 5 h (MOI = 500). (*a*) Cationic ferritin (0.5 mg/ml) was added for 1 h at 4 h postinfection and examined by EM. Electron dense, granular material in the vacuoles is the ferritin label (*arrows*). (*b*) Lgp120 was stained by immunoperoxidase cytochemistry using rabbit polyclonal anti-lgp120 IgG as primary antibody. Bars: (*a*) 360; (*b*) 100 nm.

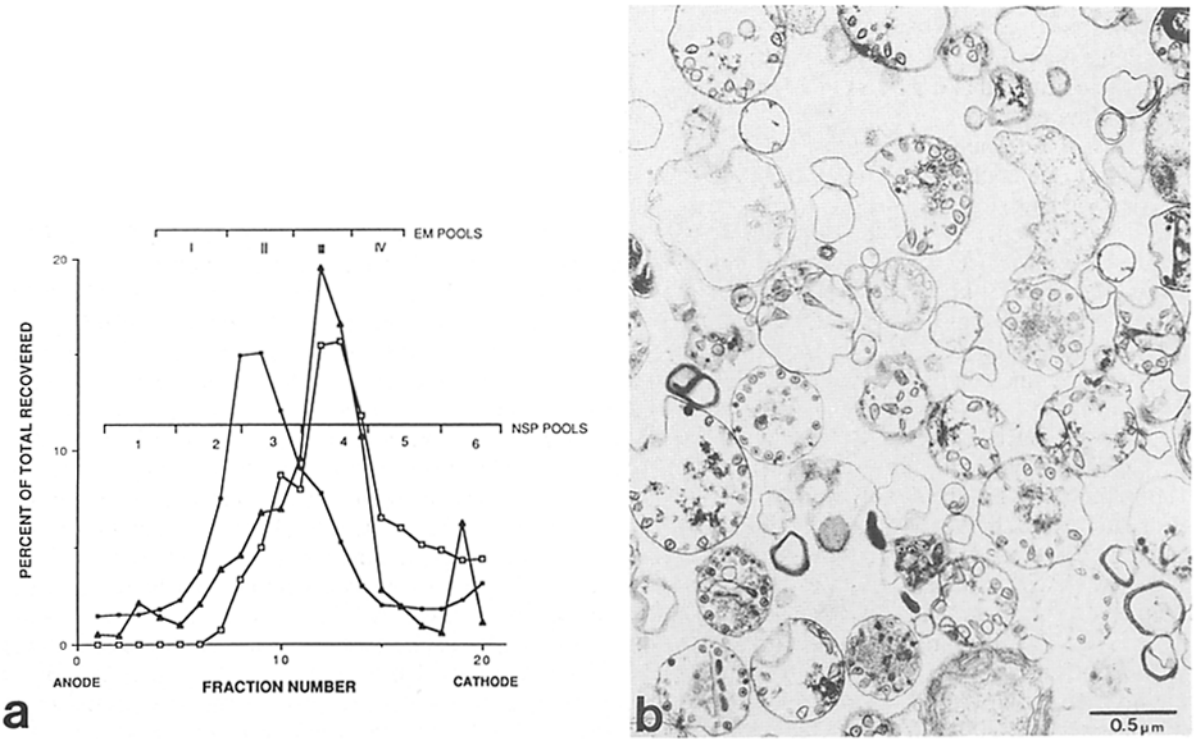

Figure 3. Resolution of CPVs by free-flow electrophoresis of alphavirus-infected CHO cells. Approximately 1 × 10^8 cells were infected with SFV for 5 h (MOI = 500) and subjected to free-flow electrophoresis as described in Materials and Methods. At 5 h postinfection, cells were pulse labeled for 2 min with [^{3}H]uridine in the presence of 2 μg/ml actinomycin D. (*a*) Lysosomes were detected by β-hexosaminidase activity (■) (Pool et al., 1983), and protein (□) by Bradford assay (1976). Newly synthesized viral RNA was detected by TCA-precipitable radioactivity (▲). Activities are expressed as the percent of total activity eluted by free-flow electrophoresis. The peak RNA fraction contained 1,870 cpm. Approximately 1.5 mg of protein was applied to the apparatus. Pools I–IV denote the fractions pooled to detect CPVs by ultrathin-section EM, and pools 1–6, for immunoprecipitation of nsPs. The pools marked were from separate, but comparable, free-flow electrophoresis experiments. (*b*) Ultrastructure of CPVs in pellet of pool II. Morphometry (see Materials and Methods) showed that 71% of the membrane in pool II was in CPVs. Note the threadlike material normally at the base of spherules is absent (e.g., Fig. 1 *c*).

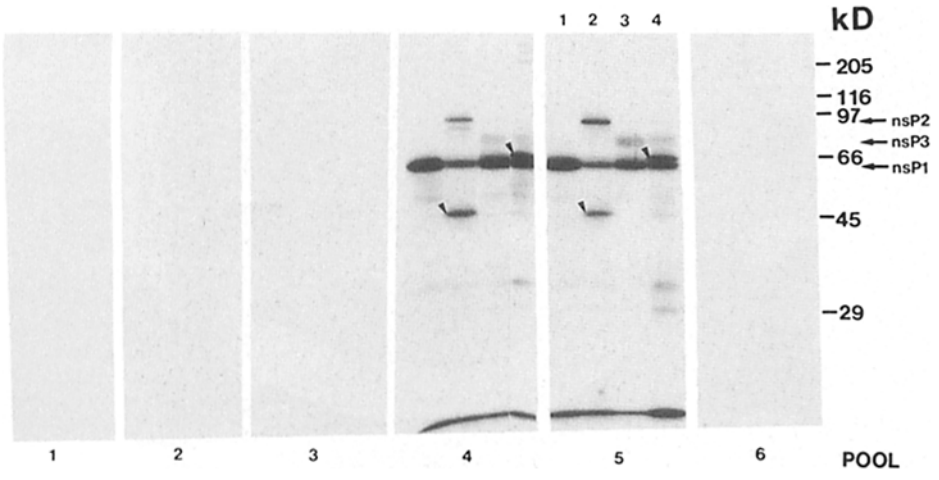

Figure 4. Immunoprecipitation of Sindbis nsPs in free-flow electrophoresis cell fractions. Sindbis-infected CHO cells (MOI = 500) were labeled with [^{35}S]methionine for 4 h, at 1 h postinfection (see Materials and Methods). Pelleted pools (Fig. 3 *a*) were solubilized in NP-40 and precipitated with polyclonal rabbit anti-nsP1, 2, 3, and 4 antisera. Immune complexes were collected and resolved on a 10% Laemmli gel. Bands in fluorogram correspond to nsPs in free-flow fractions. Six pools (1–6) were analyzed as indicated at the bottom. Samples in lanes *1–4*, labeled at the top of Pool *5*, were precipitated with anti-nsP1, 2, 3, and 4, respectively. The antibody order was the same for each of the six pools. The arrowhead in lane *2* (Pools *4* and *5*) indicates an 89-kD tryptic fragment precipitated by anti-nsP2 antiserum; the arrowhead in lane *4* (Pools *4* and *5*) indicates a 66-kD tryptic fragment precipitated by anti-nsP4 antiserum (see Results). The positions of molecular mass markers from Coomassie Blue-stained gel are shown at the right. The positions of nsP1, 2, and 3 are also indicated. Pools *1–3*, and *6* contained no detectable nsPs.

majority of nonstructural proteins were, in fact, found to cofractionate with the main protein peak, not with the lysosomes. This finding indicated that the CPVs in this preparation did not contain the enzyme.

In the precipitations, we found that nsP1 was not only precipitated by anti-nsP1, but also by anti-nsP2, anti-nsP3, and anti-nsP4 (Fig. 4). This suggested the presence of complexes between these proteins. When homogenates were trypsin treated for free-flow electrophoresis, anti-nsP2 also precipitated the nsP2 band (89 kD) and a tryptic fragment of nsP2 (42 kD) (*arrowhead*; Fig. 4, Pool *4* and *5*, lane *2*). Anti-nsP4 precipitated a band of 66 kD which probably corresponded to a tryptic fragment of nsP4 (*arrowhead*, Fig. 4, Pool *4* and *5*, lane *4*).

If CPVs were involved in RNA replication, we would have expected them not only to contain the nonstructural proteins, but also viral RNA that could be labeled in the intact cell during a short [^{3}H]uridine pulse in the presence of actinomycin D. As shown in Fig. 3 *a*, viral RNA could be easily labeled in a 2-min pulse, but it, too, was found to codistribute with the main protein peak. It was clear that by this method the isolated CPVs did not contain the viral RNA polymerase nor the replicative intermediates. Either the CPVs were not the site for RNA replication, or the RNA polymerase and replicative complexes had been lost during isolation, possibly due to the homogenization or the trypsin treatment.

Immunolocalization of RNA Polymerase

To extend our examination of the intracellular distribution of the RNA polymerase, we used immunofluorescence and ultrastructural immunocytochemistry. Initial immunoprecipitation studies on [^{35}S]methionine-labeled CHO cells established that nsP1 and 2 were detectable in CHO cells by 2 h after infection, and nsP3 and 4, which were less abundant, ~1 h later (data not shown). Only two of the anti-nsP antisera, anti-nsP3 and anti-nsP4, proved useful for immunolocalization. The two others failed to react with fixed antigens. Anti-nsP3 and 4 gave identical results in every respect and could be used interchangeably.

Immunofluorescence. Indirect immunofluorescence revealed that RNA polymerase subunits nsP3 and nsP4 were concentrated in discrete, solid spots distributed throughout the cytoplasm of the infected cells (Fig. 5). These spots did not have the rounded, vacuolar morphology typical of antigens localized to lysosomes or endosomes. In addition, while nearly all cells in the culture were infected, only a relatively small fraction showed strong staining for the RNA polymerase. The immunofluorescence results were encouraging, however, since they showed there was enough antigen for high resolution ultrastructural immunolocalization.

Immunogold-labeling in Semipermeabilized Cells. Our first ultrastructural approach relied on preparation of semi-intact cells according to the method of Beckers et al. (1987). In their method, a nitrocellulose filter is placed onto the surface of an unfixed cell monolayer. When it is removed, fragments of the plasma membrane are detached without drastically disturbing the overall morphology and architecture of the cell and its intracellular organelles. Biochemical data show that the procedure is much milder than homogenization (Simons and Virta, 1987; Beckers et al., 1987). Making holes in the plasma membrane in this way allowed us to wash out the cytosol, fix lightly with formaldehyde, and introduce antibodies and colloidal gold conjugates. As secondary antibodies we used goat anti-rabbit IgG conjugated with 5-nm gold particles.

As shown in Fig. 6 (*arrows*), the structures stained by antibodies to nsP3 and nsP4 were the fibrous, granular material that we had seen in normal thin sections extending from the CPVs into the cytosol (e.g., *large arrowheads*; Fig. 1, *b* and *c*). This material was now more easily discerned since most of the cytosol had been removed. It was revealed as a characteristic feature present on most CPVs. It seemed to be attached to the CPVs at the base of the spherules where the plug was located extending outwards as complex, fibrillar, and granular networks. In addition, labeling occurred at the base of spherules present on the plasma membrane (Fig. 6 *c*). Here it was less extensive, but again clearly connected to the spherules. Gold labeling was only seen in infected cells, it

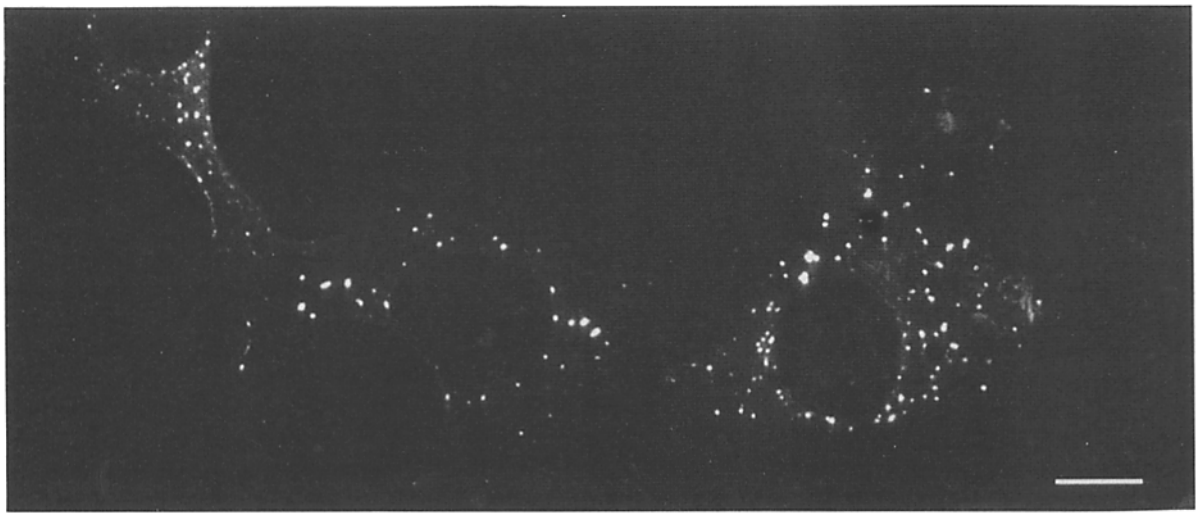

Figure 5. Indirect immunofluorescence localization of nsP3 in Sindbis-infected NIH3T3 cells. 4 h after infection (MOI = 100) cells were methanol-fixed and stained with rhodamine-conjugated goat anti-rabbit IgG. Rabbit antisera were preadsorbed to uninfected NIH3T3 cells. Bar, 190 μm.

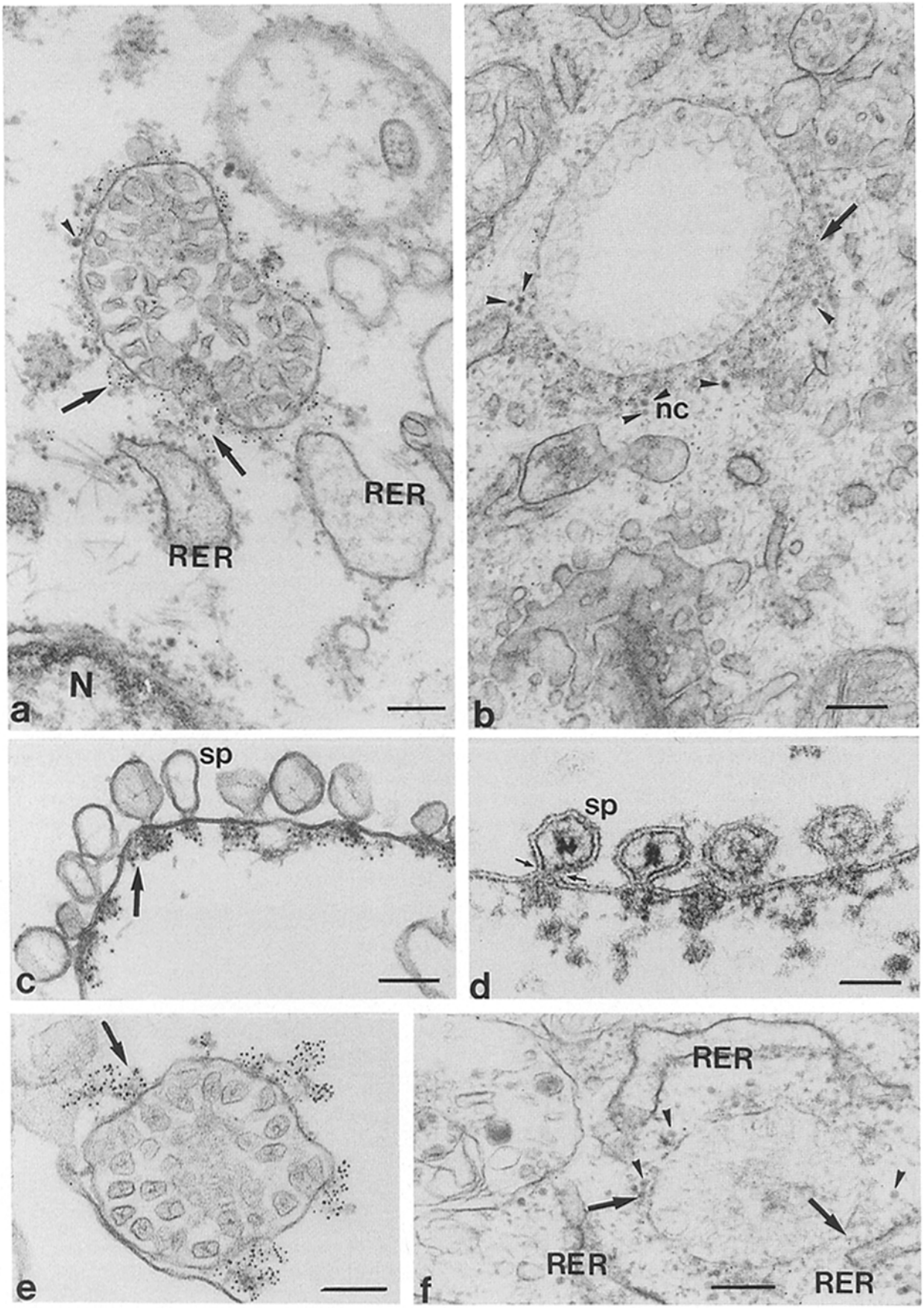
RER
RER
N
a
nc
b
sp
c
sp
d
e
RER
RER
RER
f

was absent with control antibodies, and the pattern was reproducible. Clusters of gold particles were also seen on amorphous material associated with the RER, and sometimes in free complexes without apparent membrane attachment. Association of immunogold with mitochondria and with the Golgi membranes was not observed, nor was it seen in regions of the plasma membranes devoid of spherules.

Often a close proximity between RER membranes and CPVs could be observed (Fig. 6, *a* and *f*). It was striking that the amorphous, gold-stained material appeared to form a bridge between the RER surface and the CPV, as if suspended between these two organelles. This observation was in agreement with the frequent, "next-neighbor" relationship between the two organelles noted in normal thin sections (Fig. 1 *a*). Nucleocapsids, dark spherical particles with diameters of 30 nm (*small arrowheads*, Figs. 1 *e* and 6, *a*, *b*, and *f*) were also frequently components of the meshwork.

Immunocytochemistry on Saponin-permeabilized Cells. To examine the RNA polymerase complexes further, we opened cells by saponin permeabilization as described by Brown and Farquhar (1984). The advantage of this immunocytochemical technique is less disruption of the cells and cytoplasm; the disadvantage is that the morphology of the spherules suffer from the saponin treatment. We found, however, that the preservation of CPVs was satisfactory (Fig. 6 *b*).

The antibody-staining pattern confirmed the distribution of nsP3 and nsP4 seen in the semi-intact cells. The RNA polymerase-containing structures were impressive in size, extending 800 nm from the membrane of the CPV. Numerous nucleocapsids were present within the meshwork. The connections with the RER were quite clear. In no instance did we see staining of the spherules themselves with gold although any antigens within them should have been accessible after the saponin treatment.

In double-labeling experiments nsP3 was labeled with 10-nm gold and lgp96, one of the lysosomal membrane antigens, with 5-nm gold. It was found that the viral polymerase antibodies stained the outside surface of a CPV, and the lgp96 antibodies stained the lumen and the spherules (not shown). This verified the dual nature of the CPV, it was a lysosome serving as a matrix for the viral RNA polymerase and for the replicative intermediates.

Discussion

Alphavirus infection induces at least two different types of cytopathic vacuoles: cytopathic vacuoles I and cytopathic vacuoles II. The results in this paper show that the cytopathic vacuoles I (CPVs), which appear early in infection, are modified lysosomes and endosomes. By immunocytochemistry we found that they have extensive, branched, nonmembranous structures that contain the viral RNA polymerase attached to their cytoplasmic surface at the bases of the spherules. The morphological analysis showed that the attached material also contains particulate bodies including ribosomes and nucleocapsids. Wherever spherules were observed on the plasma membrane, similar cytoplasmic ribonucleoprotein material was present, but few nucleocapsids were seen. Taken together with previous data on the CPVs (cell fractionation and autoradiography), it is evident that the material is likely to constitute the site of RNA replication in the cytoplasm of the infected cell.

The majority of the CPVs were positive for cathepsin L, lysosomal membrane proteins, and endocytic markers internalized either before or during infection. Upon cell fractionation using free-flow electrophoresis, the majority behaved like normal lysosomes. During infection, preexisting lysosomes were apparently converted into CPVs that continued to internalize endocytosed material. Particularly during the first hours of infection some CPVs appeared more prelysosomal (endosomal) in character suggesting that CPVs may originate from modified endosomes, which then proceed to become lysosomes, as do normal endosomes, At later times nearly all the lysosomes in heavily infected CHO cells were converted to CPVs.

When infected cells were permeabilized by rupturing the plasma membrane and inspected using immunocytochemistry, frequent connections between the CPVs and the RER via the RNA polymerase-containing filamentous and granular networks were observed. The close apposition of CPVs and the RER was confirmed by immunocytochemistry using fixed saponin-permeabilized cells and by standard thin-section analysis. The distance between the two membranes was often filled with extensive networks of RNA polymerase-containing material and nucleocapsids.

The origin and composition of the spherules that line the inside surface of CPV membrane, and provide a morphological hallmark for the structures, remains unknown. They clearly provide the attachment sites for the RNA polymerase-containing material, but contain no detectable parental viral RNA or RNA polymerase themselves, judging by immunocytochemistry and cell fractionation. We found that the number of CPVs and spherules correlated roughly with the MOI; small numbers of spherules were present in endosomes by 1 h after infection, whereas endosomes and lysosomes lined with spherules were observed only in late stages of infection (i.e., when superinfection was already ongoing). It remains a possibility that the spherules are, in fact, remnants of the incoming virus particles that stay associated with the endosomal and lysosomal membranes after fusion. We are in the process of determining whether the spherules contain parental nucleocapsid proteins which are known to have a relatively long half-life within the infected cell. Which cellular components they contain and why they obtain their characteristic shape and morphology is not clear.

Figure 6. Immunogold localization of nsP3 and nsP4. CHO cells were infected with Sindbis for 4.5 h (MOI = 200) and disrupted with nitrocellulose filters (*a*, *c*, and *e*) or permeabilized with 0.1% saponin (*b*, *d*, and *f*). The nsP3 and nsP4 antigens were identified using 5-nm gold-conjugated goat anti-rabbit IgG secondary antibodies and rabbit anti-nsP3 or nsP4 IgG primary antibodies. nsP4 antigens are labeled in *e* and nsP3 in *a–d* and *f*. Large arrows indicate dense granular, threadlike material anchored at base of spherules. Neighboring RER membranes in close contact with replication complexes are indicated (*a* and *f*). Small arrowheads (*a*, *b*, and *f*) show nucleocapsids (*nc*). The threads found at the base of the spherules (*sp*) on plasma membrane also contain nsPs (*c*). Bars: (*a*) 133; (*b*) 147; (*c*) 121; (*d*) 49; (*e*) 147; and (*f*) 169 nm.

The novel finding that endosomes and lysosomes may serve as a matrix for alphavirus RNA replication raises interesting functional questions. One of them concerns the mechanisms of early cytoplasmic events during virus entry. We have previously shown that SFV enters via a receptor-mediated endocytosis pathway involving acid-induced fusion of the viral membrane with the limiting membrane of endosomes. The early steps in the pathway, now known to be common to many enveloped and nonenveloped viruses (see Kielian and Helenius, 1986; Marsh, M., and A. Helenius, manuscript submitted for publication), are schematically depicted in Fig. 7. As a result of penetration, viral nucleocapsids are transferred to the cytosolic compartment. Transfer occurs rapidly and efficiently once the viruses have reached the early endosome compartment. Once in the cytosol, it is not known whether the nucleocapsid structures remain associated with the cytosolic surface of the endosome as indicated in Fig. 7 or are released free into the cytosol. The observation that RNA replication may occur on the surface of lysosomes and endosomes suggests, however, that the nucleocapsid may, indeed, remain attached and that this is the way in which the genome is transported ultimately to the cytosolic surface of the lysosomes. It is well known that virus-containing endosomes in BHK cells are delivered by membrane fusion to lysosomes asynchronously during the first 2 h after virus internalization (Kielian et al., 1986). The lysosomal membrane, or perhaps even the membrane of the endosome, may be the site where initial uncoating and translation of the viral RNA and assembly of the functional RNA polymerase takes place. Nucleocapsids may remain membrane associated as a consequence of their affinity for the COOH-terminal tail of the spike glycoprotein E2 which after fusion should be exposed on the external surface of the endosomal membrane (Helenius and Kartenbeck, 1980; Simons and Garoff, 1980).

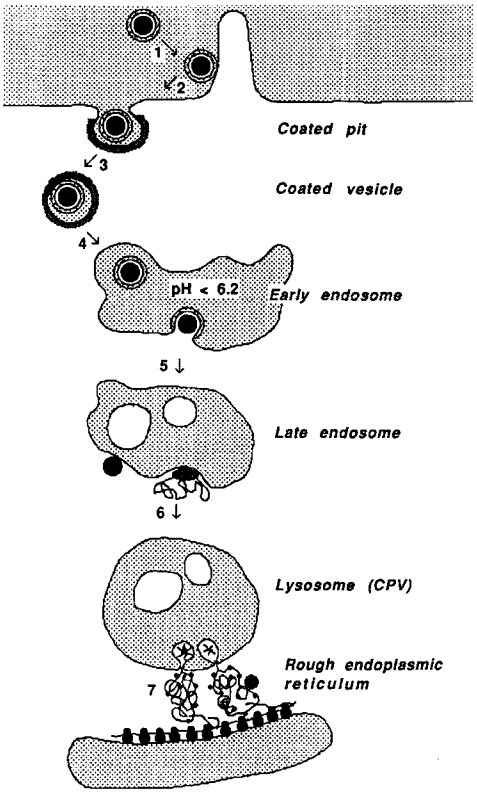

Figure 7. Schematic depiction of steps involved in alphavirus entry and early cytoplasmic events. Steps *1–5* have been established in previous work (see Kielian and Helenius, 1986; Marsh, M., and A. Helenius, manuscript submitted for publication). Steps *5–7* are hypothetical, and based on the findings of this paper. (*1*) Binding of the virus particle to proteinaceous receptors on the plasma membrane (occurs frequently to microvilli). (*2*) Lateral movement along the membrane and uptake into coated pits. (*3*) Internalization in coated vesicles. (*4*) Delivery to early endosomes, in which the pH is low enough to induce a conformational change in spike glycoproteins, and activate membrane fusion and nucleocapsid penetration into the cytosol. (*5*) The nucleocapsid remains associated with the endosomal membrane where it uncoats, and where initial translation of nonstructural proteins may begin. (*6*) The endosome fuses with a lysosome thereby transferring the replication complex to the lysosomal membrane. (*7*) A large ribonucleoprotein matrix containing the viral RNA polymerase is formed at the surface of the lysosome, a "spherule" containing part of the lysosomal membrane, cellular proteins, and possibly a remnant of the nucleocapsid is generated, and, possibly through mediation of the 26-S RNA, contacts with the RER are established. As discussed in the text, the matrix may constitute the site for RNA replication, for translation of viral proteins, and for nucleocapsid assembly.

According to this model, the site of RNA replication is primarily determined by the mode of entry. The alternative pathway, that the viral replicative complexes specifically bind to the membranes of lysosomes and endosomes later in the replicative cycle, cannot be excluded at this time, but studies in progress with microinjected infectious RNA should address this possibility. Whether the lysosomal association provides any advantages for viral replication is not known. It does suggest, however, that antiviral agents against alphaviruses could be made more effective if targeted specifically to lysosomes.

Another interesting question concerns the apparent connection between the CPVs and the endoplasmic reticulum. We would like to propose that the network which spans the space between these organelles may in fact represent a "factory" where viral RNA and proteins are synthesized, and where nucleocapsids are assembled. It is well known that one of the RNA species synthesized (the 42-S RNA [SFV]–49-S RNA [Sindbis]) serves not only as the messenger for nonstructural proteins and the template for negative-strand synthesis, but also as the genomic RNA packaged into newly formed nucleocapsids. Another RNA species (the 26-S RNA), synthesized in the same RNA polymerase–containing matrix constitutes the subgenomic messenger for the synthesis of structural proteins (Simmons and Strauss, 1972; Sawicki and Sawicki, 1980). From this messenger a polyprotein precursor (consisting of capsid and spike proteins) is translated on membrane-bound polysomes in such a way that the nucleocapsid protein (30 kD) stays in the cytosol and associates rapidly with 42-S RNA to form nucleocapsids (Scheele and Pfefferkorn, 1969; Söderlund, 1973). In contrast, the glycoproteins E1 and p62 are translocated into the RER membrane and transported to the plasma membrane where viral assembly and budding takes place (see Garoff et al., 1982; Schlesinger and Schlesinger, 1986).

The main argument that favors a functional role for the CPV–RER interaction is that the nucleocapsids must be as-

sembled from components synthesized both in the matrix, associated with the CPVs, and on the endoplasmic reticulum. Not only is the assembly of the capsid extremely rapid (it only takes 5–7 min to chase the newly synthesized capsid protein into intact, fully assembled capsids), but it is also remarkably specific. Wengler et al. (1982) have shown that, whereas the capsid protein in the infected cell specifically associates with the genomic 42-S RNA, it binds indiscriminately to virtually any single-stranded RNA in vitro. From these studies it is apparent that conditions inside the infected cell somehow favor specific interaction of the capsid protein with the 42-S RNA. Could it be that the close apposition of the CPV and the RER, and the presence of a structured matrix sterically guides association of viral 42-S RNA with the nucleocapsid protein? Newly synthesized nucleocapsid proteins may, in fact, bind to the 42-S RNA as it is being transcribed, explaining both the specificity of RNA packaging and the rapidity of nucleocapsid assembly.

We are grateful to Hans Stukenbrok and Eva Bolzau for their skillful assistance with electron microscopy; to Bruce Granger and the laboratory of Ira Mellman for many helpful discussions and for lgp and cathepsin L antisera; and to Sandy Schmid for her valuable advice during the free-flow studies. We especially thank Reef Hardy for the generous gift of nsP antisera; and Stella Hurtley, Ira Mellman, and Donald Engelman for thoughtful criticism of the manuscript.

This work was supported by a fellowship from the Jane Coffin Childs Memorial Fund for Medical Research awarded to S. Froshauer and by National Institutes of Health grant ROI GM 38346-07 awarded to A. Helenius.

Received for publication 14 July 1988, and in revised form 18 August 1988.

References

Acheson, N. H., and I. Tamm. 1967. Replication of Semliki Forest virus: an electron microscopic study. *Virology.* 32:128–143.

Balch, W. E., and J. E. Rothman. 1985. Characterization of protein transport between successive compartments of the Golgi apparatus: asymmetric properties of donor and acceptor activities in a cell-free system. *Arch. Biochem. Biophys.* 240:413–425.

Beckers, C. J. M., D. S. Keller, and W. E. Balch. 1987. Semi-intact cells permeable to macromolecules: use in reconstitution of protein transport from the endoplasmic reticulum to the Golgi complex. *Cell.* 50:523–534.

Bradford, M. 1976. A rapid and sensitive method for the quantitation of microgram quantities of protein utilizing the principle of protein dye binding. *Anal. Biochem.* 72:248–254.

Brown, W. J., and M. G. Farquhar. 1984. Accumulation of coated vesicles bearing mannose-6-phosphate receptors for lysosmal enzymes in the Golgi region of I-cell fibroblasts. *Proc. Natl. Acad. Sci. USA.* 81:5135–5139.

Chamberlain, J. P. 1979. Fluorographic detection of radioactivity in polyacrylamide gels with water-soluble fluor, sodium salicylate. *Anal. Biochem.* 98: 132–135.

Clewley, J. P., and S. I. T. Kennedy. 1976. Purification and polypeptide composition of Semliki Forest virus RNA polymerase. *J. Gen. Virol.* 32:395–411.

Dunn, W. A., A. L. Hubbard, and N. N. Aronson. 1980. Low temperature selectively inhibits fusion between pinocytic vesicles and lysosomes during heterophagy of ^{125}I-asialofetuin by perfused rat liver. *J. Biol. Chem.* 255: 5971–5978.

Friedman, R. M., J. G. Levin, P. M. Grimley, and I. K. Berezesky. 1972. Membrane-associated replication complex in arbovirus infection. *J. Virol.* 10:504–515.

Fuller, S. D. 1987. The T-4 envelope of Sindbis virus is organized by interaction with a complementary T-3 capsid. *Cell.* 48:923–934.

Garoff, H., C. Kondor-Koch, and H. Riedel. 1982. Structure and assembly of alphavirus. *Curr. Top. Microbiol. Immunol.* 99:1–49.

Gomatos, P. J., L. Kääriäinen, S. Keränen, M. Ranki, and D. L. Sawicki. 1980. Semliki Forest virus replication complex capable of synthesizing 42S and 26S nascent RNA chains. *J. Gen. Virol.* 49:61–69.

Green, S., K.-P. Zimmer, G. Griffiths, and I. Mellman. 1987. Kinetics of intracellular transport and sorting of lysosomal membrane and plasma membrane proteins. *J. Cell Biol.* 105:1227–1240.

Grimley, P. M., I. K. Berezesky, and R. M. Friedman. 1968. Cytoplasmic structures associated with an arbovirus infection: loci of viral ribonucleic acid synthesis. *J. Virol.* 2:1326–1338.

Grimley, P. M., J. G. Levin, I. K. Berezesky, and R. M. Friedman. 1972. Specific membranous structures associated with the replication of Group A arboviruses. *J. Virol.* 10:492–503.

Hardy, W. R., and J. E. Strauss. 1988. Processing of nonstructural polyproteins of Sindbis virus: study of the kinetics in vivo using monospecific antibodies. *J. Virol.* 62:998–1007.

Harms, E., H. Kern, and J. A. Schneider. 1980. Human lysosomes can be purified from diploid skin fibroblasts by free-flow electrophoresis. *Proc. Natl. Acad. Sci. USA.* 77:6139–6143.

Hawley, D. M., K. C. Tsou, and M. E. Hodes. 1981. Preparation, properties and uses of two fluorogenic substrates for the detection of 5′ (venom) and 3′ (spleen) nucleotide phosphodiesterases. *Anal. Biochem.* 117:18–23.

Helenius, A., and J. Kartenbeck. 1980. The effects of octylglucoside on the Semliki Forest virus membrane: evidence for a spike protein–nucleocapsid interaction. *Eur. J. Biochem.* 106:613–618.

Helenius, A., J. Kartenbeck, K. Simons, and E. Fries. 1980. On the entry of Semliki Forest virus in BHK-21 cells. *J. Cell Biol.* 84:404–420.

Helenius, A., M. Marsh, and J. White. 1982. Inhibition of Semliki Forest virus penetration by lysosomotropic weak bases. *J. Gen. Virol.* 58:47–61.

Kääriäinen, L., K. Simons, and C. von Bonsdorff. 1969. Studies of Semliki Forest virus subviral components. *Ann. Med. Exp. Biol. Fenn.* 47:235–248.

Keränen, S., and L. Ruohonen. 1983. Nonstructural proteins of Semliki Forest virus: synthesis, processing and stability in infected cells. *J. Virol.* 47:505–515.

Kielian, M., and A. Helenius. 1986. Entry of alphaviruses. *In* The Togaviridae and Flaviviridae. S. Schlesinger and M. J. Schlesinger, editors. Plenum Press, New York. 91–119.

Kielian, M. C., S. Keränen, L. Kääriäinen, and A. Helenius. 1984. Membrane fusion mutants of Semliki Forest virus. *J. Cell Biol.* 98:139–145.

Kielian, M. C., M. Marsh, and A. Helenius. 1986. Kinetics of endosome acidification detected by mutant and wildtype Semliki Forest virus. *EMBO (Eur. Mol. Biol. Organ.) J.* 5:3103–3109.

Laemmli, U. K. 1970. Cleavage of structural proteins during the assembly of the head of bacteriophage T4. *Nature (Lond.).* 227:680–685.

Lewis, V., S. A. Green, M. Marsh, P. Vihkko, A. Helenius, and I. Mellman. 1985. Glycoproteins of the lysosomal membrane. *J. Cell Biol.* 100:1839–1847.

Lopez, S., J. R. Bell, E. G. Strauss, and J. H. Strauss. 1985. The nonstructural proteins of Sindbis virus as studied with an antibody specific for the C terminus of the nonstructural readthrough polyprotein. *Virology.* 141:235–247.

Marsh, M., E. Bolzau, and A. Helenius. 1983. Penetration of Semliki Forest virus from acidic prelysosomal vacuoles. *Cell.* 32:931–940.

Marsh, M., G. Griffiths, G. E. Dean, I. Mellman, and A. Helenius. 1986. Three-dimensional structure of endosomes in BHK-21 cells. *Proc. Natl. Acad. Sci. USA.* 83:2899–2903.

Marsh, M., S. Schmid, H. Kern, E. Harms, P. Male, I. Mellman, and A. Helenius. 1987. Rapid analytical and preparative isolation of functional endosomes by free-flow electrophoresis. *J. Cell Biol.* 104:875–886.

McLean, I. W., and P. K. Nakane. 1974. Periodate-lysine paraformaldehyde fixative. A new fixative for immunoelectron microscopy. *J. Histochem. Cytochem.* 22:1077–1083.

Nilsson, J., T. Ksiazek, and J. Thyberg. 1983. Endocytosis of cationic and anionic proteins in cultivated arterial smooth muscle cells. *Exp. Cell Res.* 143: 359–365.

Pool, R. R., K. M. Maurey, and B. Storrie. 1983. Characterization of pinocytic vesicles from CHO cells: resolution of pinosomes from lysosomes by analytical centrifugation. *Cell Biol. Int. Rep.* 7:361–367.

Ranki, M., and L. Kääriäinen. 1979. Solubilized RNA replication complex from Semlike Forest virus–infected cells. *Virology.* 98:298–307.

Sawicki, D. L., and S. G. Sawicki. 1980. Short-lived minus-strand polymerase for Semliki Forest virus. *J. Virol.* 34:108–118.

Scheele, C. H., and E. R. Pfefferkorn. 1969. Kinetics of incorporation of structural proteins into Sindbis virus. *J. Virol.* 3:369–375.

Schlesinger, M. J., and S. Schlesinger. 1986. Formation and assembly of alphavirus glycoproteins. *In* The Togaviridae and Flaviviridae. S. Schlesinger and M. J. Schlesinger, editors. Plenum Press, New York. 121–148.

Schmid, S. L., R. Fuchs, P. Male, and I. Mellman. 1988. Two distinct subpopulations of endosomes involved in membrane recycling and transport to lysosomes. *Cell.* 52:73–83.

Simmons, D. T., and J. H. Strauss. 1972. Replication of Sindbis virus II: multiple forms of double-stranded RNA isolated from infected cells. *J. Mol. Biol.* 71:615–631.

Simons, K., and H. Garoff. 1980. The budding mechanisms of enveloped animal viruses. *J. Gen. Virol.* 50:1–21.

Simons, K., and H. Virta. 1987. Perforated MDCK cells support intracellular transport. *EMBO (Eur. Mol. Biol. Organ.) J.* 6:2241–2247.

Söderlund, H. 1973. Kinetics of formation of the Semliki Forest virus nucleocapsid. *Intervirology.* 1:354–361.

Strauss, E. G., and J. H. Strauss. 1986. Structure and replication of the alphavirus genome. *In* The Togaviridae and Flaviviridae. S. Schlesinger and M. J. Schlesinger, editors. Plenum Press, New York. 35–90.

Strauss, E. G., C. M. Rice, and J. H. Strauss. 1983. Sequence coding for the alphavirus nonstructural proteins is interrupted by an opal termination codon. *Proc. Natl. Acad. Sci. USA.* 80:5271–5275.

Ukkonen, P., V. Lewis, M. Marsh, A. Helenius, and I. Mellman. 1986. Trans-

port of macrophage Fc receptors and Fc receptor-bound ligands to lysosomes. *J. Exp. Med.* 163:952–971.

Weibel, E. R. 1969. Stereological principles for morphometry in electron microscopic cytology. *Int. Rev. Cytol.* 26:235–302.

Wengler, G., U. Boege, G. Wengler, H. Bischoff, and K. Wahn. 1982. The core protein of the alphavirus Sindbis virus assembles into core-like nucleoproteins with the viral genome RNA and with other single-stranded nucleic acids in vitro. *Virology.* 118:401–410.